

Metabolic Endotoxemia Initiates Obesity and Insulin Resistance

Patrice D. Cani,^{1,2} Jacques Amar,³ Miguel Angel Iglesias,¹ Marjorie Poggi,⁴ Claude Knauf,¹ Delphine Bastelica,⁴ Audrey M. Neyrinck,² Francesca Fava,⁵ Kieran M. Tuohy,⁵ Chantal Chabo,¹ Aurélie Waget,¹ Evelyne Delmée,² Béatrice Cousin,⁶ Thierry Sulpice,⁷ Bernard Chamontin,³ Jean Ferrières,³ Jean-François Tanti,⁸ Glenn R. Gibson,⁵ Louis Casteilla,⁶ Nathalie M. Delzenne,² Marie Christine Alessi,⁴ and Rémy Burcelin¹

Diabetes and obesity are two metabolic diseases characterized by insulin resistance and a low-grade inflammation. Seeking an inflammatory factor causative of the onset of insulin resistance, obesity, and diabetes, we have identified bacterial lipopolysaccharide (LPS) as a triggering factor. We found that normal endotoxemia increased or decreased during the fed or fasted state, respectively, on a nutritional basis and that a 4-week high-fat diet chronically increased plasma LPS concentration two to three times, a threshold that we have defined as metabolic endotoxemia. Importantly, a high-fat diet increased the proportion of an LPS-containing microbiota in the gut. When metabolic endotoxemia was induced for 4 weeks in mice through continuous subcutaneous infusion of LPS, fasted glycemia and insulinemia and whole-body, liver, and adipose tissue weight gain were increased to a similar extent as in high-fat-fed mice. In addition, adipose tissue F4/80-positive cells and markers of inflammation, and liver triglyceride content, were increased. Furthermore, liver, but not whole-body, insulin resistance was detected in LPS-infused mice. CD14 mutant mice resisted most of the LPS and high-fat diet-induced features of metabolic diseases. This new finding demonstrates that metabolic endotoxemia dysregulates the inflammatory tone and triggers body weight gain and diabetes. We conclude that the LPS/CD14 system sets the tone of insulin sensitivity and the onset of diabetes and obesity. Lowering plasma LPS concentration could be a potent strategy for the control of metabolic diseases. *Diabetes* 56:1761–1772, 2007

From the ¹Institute of Molecular Medicine, I2MR Toulouse, France; the ²Unité Pharmacocinétiques, Metabolism, Nutrition, and Toxicology-73/69, Université catholique de Louvain, Brussels, Belgium; the ³Institut National de la Santé et de la Recherche Médicale (INSERM) 558, Toulouse, France; ⁴INSERM U 626, Marseille, France; the ⁵Food Microbial Sciences Unit, Department of Food Biosciences, University of Reading, Reading, U.K.; the ⁶Unité Mixte de Recherche 5241, Centre National de la Recherche Scientifique, Université Paul Sabatier, Toulouse, France; ⁷Physiogenex S.A.S., Labège Innopole, France; and ⁸INSERM U 568, Nice, France.

Address correspondence and reprint requests to Rémy Burcelin, I2MR U858, IFR 31, Hôpital Rangueil, BP 84225, Toulouse 31432 Cedex 4, France. E-mail: burcelin@toulouse.inserm.fr.

Received for publication 24 October 2006 and accepted in revised form 13 April 2007.

Published ahead of print at <http://diabetes.diabetesjournals.org> on 24 April 2007. DOI: 10.2337/db06-1491.

P.D.C., J.A., and M.A.I. contributed equally to this article.

IKK, inhibitor of κ B kinase; IL, interleukin; LPS, lipopolysaccharide; PAI, plasminogen activator inhibitor; TLR4, toll-like receptor 4; TNF, tumor necrosis factor.

© 2007 by the American Diabetes Association.

The costs of publication of this article were defrayed in part by the payment of page charges. This article must therefore be hereby marked "advertisement" in accordance with 18 U.S.C. Section 1734 solely to indicate this fact.

The outbreak of a fat-enriched diet in Western countries is becoming a problem of the utmost importance. Obesity is the result of a complex interaction between genetic and environmental factors. Among the latter, changes in eating habits to increase fat intake are involved in the increased occurrence of metabolic diseases, such as obesity and diabetes, which are bearing features of the metabolic syndrome. The major metabolic consequence of a high-fat diet is that insulin action and the regulatory mechanisms of body weight are impaired through a well-described lipotoxic effect (1). In addition, it has been recently determined that obesity and insulin resistance are associated with low-grade chronic systemic inflammation (2). In models of diet-induced and genetic obesity, the adipose tissue presents increased expression and content of proinflammatory cytokines such as tumor necrosis factor (TNF)- α (3,4), interleukin (IL)-1 (3,4), and IL-6 (4). This cytokine production is then deleterious for muscle insulin action; for example, TNF- α has been shown to cause insulin resistance by increasing serine phosphorylation on insulin receptor substrate-1 (5), leading to its inactivation. The consequent insulin resistance will favor hyperinsulinemia and excessive hepatic and adipose tissue lipid storage. However, while extensive research is dedicated to the effects of an inflammatory reaction on energy metabolism, the triggering factor linking inflammation to high-fat diet-induced metabolic syndrome remains to be determined. Recently, it has been shown that nutritional fatty acids activate toll-like receptor-4 (TLR4) signaling in adipocytes and macrophages and that the capacity of fatty acids to induce inflammatory signaling in adipose cells or tissue and macrophages is blunted in the absence of TLR4 (6). Furthermore, adipose tissue lipolysis, from hypertrophied adipocytes, could serve as a naturally occurring ligand for TLR4 to induce inflammation (7). In addition, TLR4 mRNA concentration was induced during adipocyte differentiation, further enhancing free fatty acid-induced inflammation (8).

A very encouraging and innovative hypothesis has recently been proposed whereby the microbial ecology in humans could be an important factor affecting energy homeostasis (i.e., individuals predisposed to obesity may have gut microbial communities that would favor the occurrence of the metabolic diseases) (9–11). Although

the proposed mechanism was to promote a more efficient extraction and/or storage of energy from a given diet, the impact of microbiota on the occurrence of a low-tone inflammatory status was not determined. However, another study recently showed that antibiotic treatment partially protects against type 1 diabetes in a diabetes-prone rat developing insulinitis (12). The authors proposed that altering the gut microbiota composition by antibiotic treatment had reduced the antigenic load and hence the inflammatory reaction that had potentially led to pancreatic β -cell destruction. In that respect, we have been looking for a factor of microbial origin that would trigger and maintain a low-tone continuous inflammatory state when feeding on a high-fat diet. We hypothesized that the bacterial lipopolysaccharide (LPS) from the Gram-negative intestinal microbiota would fulfill all the prerequisites to be eligible. Thus, endogenous LPS is 1) continuously produced in the gut by the death of Gram-negative bacteria and physiologically translocated into intestinal capillaries through a TLR4-dependent mechanism (13); 2) transported from the intestine toward target tissues by a mechanism facilitated by lipoproteins, notably chylomicrons freshly synthesized from epithelial intestinal cells in response to a high-fat diet (14); and 3) triggers the secretion of proinflammatory cytokines when it binds to the complex of mCD14 and the TLR4 at the surface of innate immune cells (15,16). Therefore, we aimed to demonstrate that LPS would be an early factor in the triggering of high-fat diet-induced metabolic diseases.

RESEARCH DESIGN AND METHODS

Twelve-week-old male C57bl6/J mice (Charles River, Brussels, Belgium) and CD14 mutant mice bred in a C57bl6 background (Jackson Laboratory, Bar Harbor, ME) were housed in a controlled environment (inverted 12-h daylight cycle, lights off at 10:00 A.M.) with free access to food and water. All of the following animal experimental procedures were validated by the local ethical committee of the Ranguel Hospital and by the Université catholique de Louvain Animal Ethical Committee.

Mice were fed a control (A04, Villemoisson sur Orge, France) or a high-fat, carbohydrate-free diet for 2 or 4 weeks following protocols. The diet contained 72% fat (corn oil and lard), 28% protein, and <1% carbohydrate as energy content (17). In a subset of mice, obesity and diabetes were induced by a high-fat diet and mice killed after 4 or 24 weeks.

Energy intake measurements. Energy intake was recorded twice weekly for 4 weeks, two mice per cage. Pellets and spillage were weighed separately. The mean value for the weekly assessment was calculated. This method was performed similarly for all assessments.

Surgical procedures, infusions, and isotope measurements. Mice were implanted subcutaneously with an osmotic minipump (Alzet Model 2004; Alza, Palo Alto, CA) as previously described (17). The pumps were filled either with NaCl (0.9%) or LPS (from *Escherichia coli* 055:B5; Sigma, St. Louis, MO) to infuse $300 \mu\text{g} \cdot \text{kg}^{-1} \cdot \text{day}^{-1}$ for 4 weeks. For the clamp studies, an intrafemoral catheter was indwelled as previously described (18). Insulin sensitivity was assessed by the euglycemic-hyperinsulinemic clamp as described (19). Briefly, 6-h-fasted mice were infused with insulin at a rate of 18 (pharmacological, to assess whole-body insulin sensitivity) or 1 (physiological, to assess the effect of insulin on the inhibition of endogenous glucose production) $\text{mU} \cdot \text{kg}^{-1} \cdot \text{min}^{-1}$ for 3 h. For glucose turnover measurements, $\text{D}-(^3\text{H})\beta$ -glucose (Perkin Elmer, Boston, MA) was simultaneously infused at rate of $30 \mu\text{Ci}/\text{kg}$, as described (17). $\text{D}-(^3\text{H}-3)$ -glucose enrichments were determined from total blood after deproteinization by a $\text{Zn}(\text{OH})_2$ precipitate, as described (19). To assess whether CD14 mice were sensitive to LPS-induced inflammation, fasted mice were continuously infused with LPS ($0.5 \text{ mg} \cdot \text{kg}^{-1} \cdot \text{h}^{-1}$) for 3 h. Liver and white adipose tissue were collected and frozen at -80°C .

Glucose and LPS tolerance tests. Intraperitoneal or oral glucose tolerance tests were performed as follows: 6-h-fasted mice were injected with glucose into the peritoneal cavity (1 g/kg glucose, 20% glucose solution) or by gavage (3 g/kg glucose, 66% glucose solution). Blood glucose was determined with a glucose meter (Roche Diagnostics) on $3.5 \mu\text{l}$ blood collected from the tip of the tail vein. A total of $20 \mu\text{l}$ blood was sampled 30 min before and 15 or 30 min after the glucose load to assess plasma insulin concentration. An LPS

tolerance test was performed as follows. Fasted mice were gavaged by LPS ($300 \mu\text{g}/\text{kg}$) diluted in water or corn oil ($100 \mu\text{l}$) or without LPS. Blood was collected from the tip of the tail vein before and 30 min after gavage. Plasma was separated and frozen.

Microbial enumeration in intestinal content by fluorescent in situ hybridization. The caecal contents collected post mortem from mice were stored at -80°C . Samples were thawed on ice and diluted 1:10 in sterile ice-cold 0.1 mol/l PBS, pH 7.0. The suspension was homogenized by pipetting and centrifuged at $3,500g$ for 15 min to remove particulate matter. The supernatant containing the bacterial cells was fixed overnight in 4% (wt/vol) paraformaldehyde. The bacterial cells were then washed and resuspended twice in sterile PBS and finally stored in 50% ethanol in PBS at -20°C until hybridization with appropriate molecular probes targeting specific regions of 16S rRNA. The probes used were EREC 482, Bac303, MIB 661, Lab158, Bif164, SRB 687, and probe D specific for the *Eubacterium rectale/Clostridium coccooides* group, *Bacteroides* species, mouse intestinal bacteria, Lactobacilli/Enterococci, *Bifidobacterium* species, sulfate-reducing bacteria, and the *Enterobacteriaceae*, respectively. The nucleic acid stain DAPI (4',6-diamidino-2-phenylindole) was used for total bacterial counts. The DNA probes were tagged with the Cy3 fluorescence dye so that the hybridized samples could be examined using fluorescence microscopy, as described previously (20). Results were expressed as \log_{10} (bacterial cells per gram caecal content wet weight).

Real-time quantitative PCR. Total RNAs from liver, muscle, and white adipose tissue were prepared using TriPure reagent (Roche, Basel, Switzerland) as described (21). PCRs were performed using an ABI PRISM 5700 Sequence Detection System instrument and software (Applied Biosystems, Foster City, CA) as described (21). Primer sequences for the targeted mouse genes are available upon request (E-mail: patrice.cani@uclouvain.be).

Western blots. One hundred milligrams of liver were homogenized in lysis buffer, and the proteins were separated onto a polyacrylamide gel and transferred to polyvinylidene fluoride membrane, as described (17). The membranes were incubated overnight at 4°C with the indicated antibody of nuclear factor κB -p65 (Cell signaling, Saint Quentin Yvelines, France) and inhibitor of κB kinase β -P (Santa Cruz, Le Perray en Yvelines, France). The binding of the specific primary antibody was quantified as described (17).

Adipose tissue morphometry and F4/80 staining. The mean relative proportion of adipocytes was estimated by a point-counting technique, on paraffin-embedded hematoxylin eosine staining counterstained sections of subcutaneous tissue. The number of adipocytes per microscopical field (density) was determined at a magnification of $\times 200$. Total count ranged from 2,300 to 6,600 cells per condition. The mean surface area of the adipocytes (μm^2) was calculated using image analyzer software (Visilog 6, Courtaboeuf, France). Each adipocyte was manually delineated, and 700–1,000 adipocytes per condition were assessed. F4/80 staining was performed as follows. Ethanol-fixed, paraffin-embedded adipose tissue sections were deparaffinized and rehydrated. Sections were blocked in normal serum and incubated overnight with primary rat anti-mouse F4/80 monoclonal antibody (1/1,000; Serotec, Oxford, U.K.). Endogenous horseradish peroxidase activity was quenched with incubation with 3% hydrogen peroxide for 20 min. Secondary antibody staining was performed using goat anti-rat biotinylated Ig Ab (1/500, 30 min, room temperature) and streptavidin horseradish peroxidase conjugated (1/500, 30 min, room temperature) and detected with 3,3'-diaminobenzidine. Sections were counterstained with hematoxylin before dehydration and coverslip placement. The number of F4/80-positive cells per microscopical field was calculated and divided by the total number of adipocytes in sections. Twelve to 17 fields were counted per condition.

Liver histology. A fraction of the main liver lobe was fixed-frozen in Tissue-tek in liquid nitrogen-cold isopentane. For the detection of neutral lipids, frozen sections were sliced and stained with the oil red O, using 0.5% oil red O dissolved in propylene glycol for 10 min at 60°C . The sliced sections were then counterstained.

Biochemical analyses. Plasma LPS determinations in the mouse were performed using a kit based upon a *Limulus* amoebocyte extract (LAL kit; Cambrex BioScience, Walkersville, MD). Samples were diluted 1/40 to 1/80 and heated during 10 min at 70°C . Internal control of recovery calculation was included in the assessment. Plasma insulin concentrations were determined in $5 \mu\text{l}$ of plasma using an enzyme-linked immunosorbent assay kit (Mercodia, Upsala, Sweden), following manufacturer's instructions. Liver triglyceride was determined as follows: total neutral lipids were extracted from 30 to 50 mg liver in $\text{CHCl}_3\text{-MeOH}$ (2:1). The organic extracts were air dried, reconstituted in isopropanol, and assayed for triglycerides by measuring the glycerol produced after enzymatic hydrolysis of triglycerides using a commercial kit (Triglycerides GPO Trinder; Sigma, Lyon, France).

Statistical analysis. Results are presented as means \pm SE. Statistical significance of differences was analyzed by one-way ANOVA followed by post hoc (Bonferroni's multiple comparison test) using GraphPad Prism version

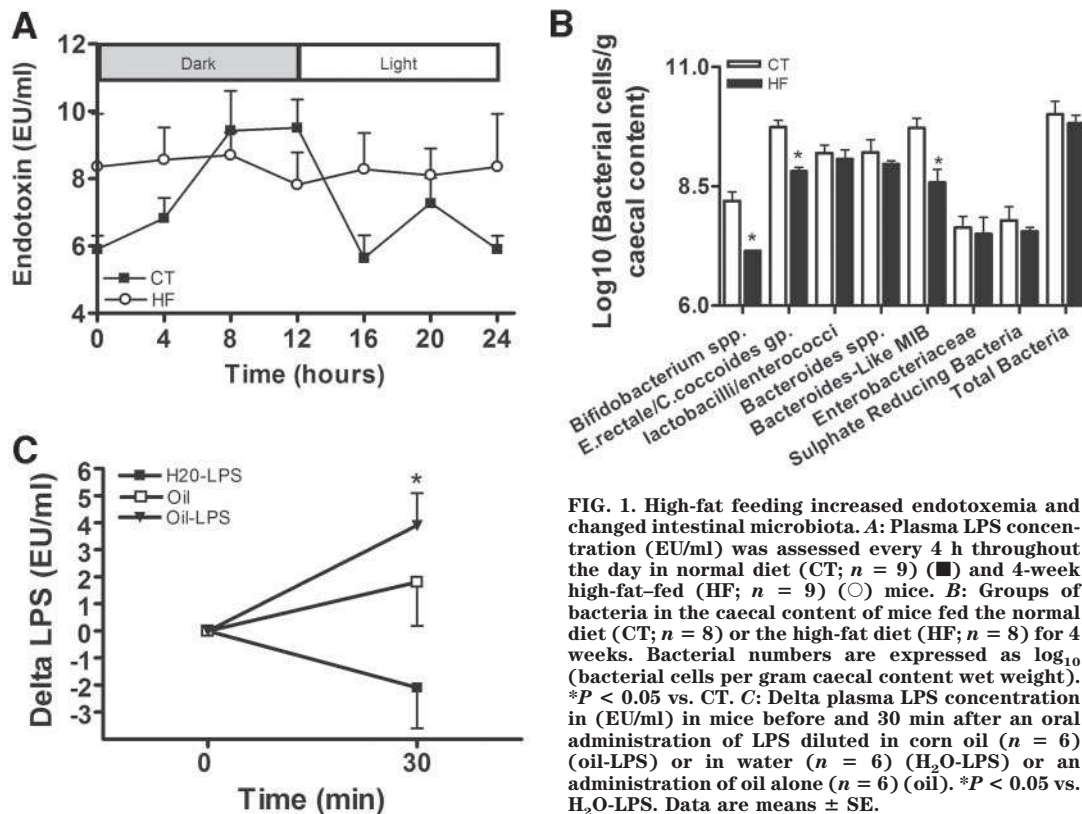


FIG. 1. High-fat feeding increased endotoxemia and changed intestinal microbiota. **A:** Plasma LPS concentration (EU/ml) was assessed every 4 h throughout the day in normal diet (CT; $n = 9$) (■) and 4-week high-fat-fed (HF; $n = 9$) (○) mice. **B:** Groups of bacteria in the caecal content of mice fed the normal diet (CT; $n = 8$) or the high-fat diet (HF; $n = 8$) for 4 weeks. Bacterial numbers are expressed as \log_{10} (bacterial cells per gram caecal content wet weight). * $P < 0.05$ vs. CT. **C:** Delta plasma LPS concentration in (EU/ml) in mice before and 30 min after an oral administration of LPS diluted in corn oil ($n = 6$) (oil-LPS) or in water ($n = 6$) (H₂O-LPS) or an administration of oil alone ($n = 6$) (oil). * $P < 0.05$ vs. H₂O-LPS. Data are means \pm SE.

4.00 for Windows (GraphPad Software, San Diego, CA). Data with different superscript letters and * or § are significantly different at $P < 0.05$, according to the post hoc ANOVA statistical analysis.

RESULTS

High-fat diet increased endotoxemia. Because LPS is an important component of lipoprotein (14), and dyslipidemia an important feature of metabolic disease, we studied the high-fat diet-fed mouse to determine the effect of a high-fat diet on the occurrence of plasma LPS concentration. We determined whether plasma LPS could be a physiological regulating factor dependent on the feeding status and measured the endotoxemia throughout the day. Our data show the existence of diurnal variations of plasma LPS concentration, which reaches a zenith at the end of the dark, feeding period (Fig. 1A). Furthermore, a short time (4 weeks) of high-fat feeding caused a disruption of this cycle, with endotoxemia remaining high throughout the whole day. This increase was still 10–50 times lower than values that could be reached during septicemia or other infections (22). Hence, we defined it as a metabolic endotoxemia. To determine whether a high-fat diet could bring about a modification within the intestinal microbiota, which might account for the observed increased levels of plasma LPS and, thus, metabolic endotoxemia, we characterized and quantified the main bacterial families of cecal microbiota in high-fat-fed and control mice. Maintenance of the mice on a high-fat diet for 4 weeks resulted in a significant modulation of dominant bacterial populations within the intestinal microbiota. Numbers of the newly recognized Gram-negative operating taxonomic unit, *Bacteroides*-like mouse intestinal bacteria (covered by the MIB661 probe), which reside within the *Cytophaga-Flavobacter-Bacteroides* phylum, were significantly reduced in animals fed the high-fat diet. These bacteria are closely related to the *Bacteroides*

Prevotella group but are not enumerated by the *Bacteroides* probe Bac303. Bacteria enumerated by the MIB661 probe are the most numerous Gram-negative bacteria within the mouse intestinal tract and, together with the *Eubacterium rectale-Clostridium coccoides* group, constitute the dominant members of the mouse intestinal microbiota (23). Numbers of the *Eubacterium rectale-Clostridium coccoides* group and bifidobacteria were also significantly lower in animals fed the high-fat diet compared with controls (Fig. 1B). Interestingly, these bacterial families are predominantly Gram positive. Second, we assessed whether exogenous LPS could be absorbed by a high-fat diet. We orally administered LPS diluted in oil or water to mice and found that endotoxemia rose after the LPS-oil mixture administration only (Fig. 1C). In addition, administration of oil alone also tended to increase endotoxemia. Therefore, both sets of experiments suggested that exogenous and endogenous LPS origin participate toward increased endotoxemia in the presence of a lipid-rich diet.

Chronic experimental metabolic endotoxemia induces obesity, diabetes, and liver insulin resistance. Therefore, to causally link high-fat diet-increased plasma LPS concentration to metabolic disease, we mimicked the metabolic endotoxemia obtained during a 4-week high-fat feeding by implanting a subcutaneous osmotic minipump and performing a chronic continuous subcutaneous infusion of LPS for 1 month (Fig. 2A). A 72% high-fat-enriched diet increased endotoxemia 2.7-fold when compared with control fed mice. Interestingly, this increase was modest 1.4-fold when the mice were fed with a 40% high-fat-enriched diet. Therefore, we performed all studies with the 72% high-fat-enriched diet. Fasted glycemia was higher in chronic LPS-infused compared with saline-infused mice (Fig. 2B). Similarly, 15 min following oral glucose chal-

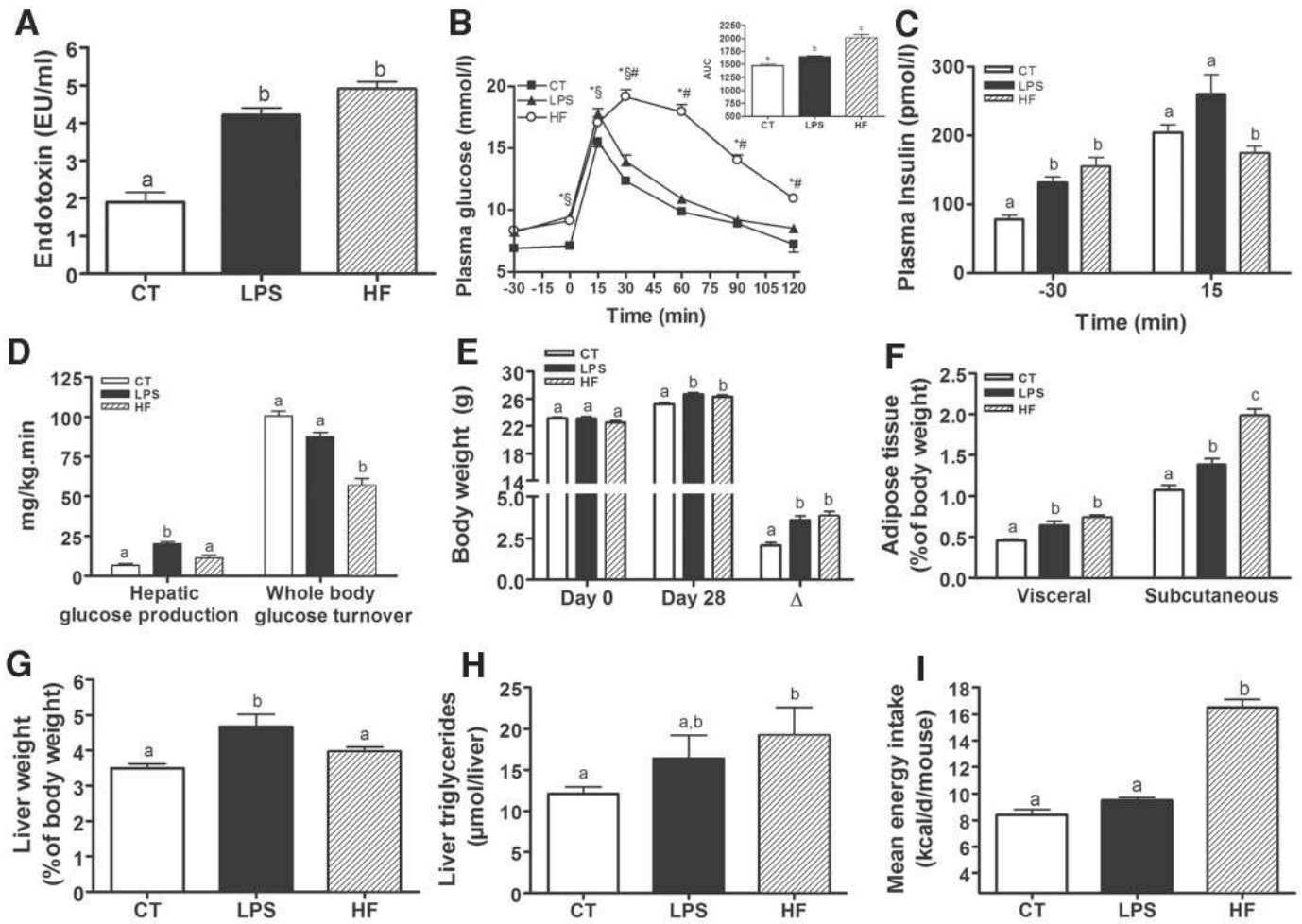


FIG. 2. Chronic experimental metabolic endotoxemia induces obesity and diabetes. *A*: Plasma endotoxin concentration (EU/ml) in WT mice infused with saline (CT; $n = 18$) or LPS ($n = 18$) for 4 weeks using subcutaneous osmotic pumps and compared with mice fed a high-fat diet for 4 weeks (HF; $n = 18$). *B*: Plasma glucose (mmol/l) following an oral glucose load (3 g/kg) in control (CT; $n = 24$), LPS ($n = 13$), or high-fat diet (HF; $n = 24$) mice. The inset represents the area under curve for each group. * $P < 0.05$ vs. CT; §LPS vs. CT; #HF vs. LPS. *C*: Plasma insulin (pmol/l) concentrations 30 min before (-30) and 15 min after (15) an oral glucose load in control (CT; $n = 24$), LPS ($n = 13$), or high-fat diet-fed (HF; $n = 24$) mice. *D*: Hepatic glucose production and whole-body glucose turnover rates ($\text{mg} \cdot \text{kg}^{-1} \cdot \text{min}^{-1}$) in control (CT; $n = 5$), LPS ($n = 5$), or high-fat diet-fed (HF; $n = 5$) mice. *E*: Body weight (g) before (day 0) and after a 28-day treatment period (day 28) and body weight gain (Δ) in control (CT; $n = 26$), LPS ($n = 21$), or high-fat diet-fed (HF; $n = 34$) mice. *F*: Visceral and subcutaneous adipose tissue weight (percentage of body weight) in control (CT; $n = 26$), LPS ($n = 21$), or high-fat diet-fed (HF; $n = 34$) mice. *G*: Liver weight (percentage of body weight) in control (CT; $n = 26$), LPS ($n = 21$), or high-fat diet-fed (HF; $n = 34$) mice. *H*: Liver triglycerides ($\mu\text{mol/liver}$) in control (CT; $n = 12$), LPS ($n = 9$), or high-fat diet-fed (HF; $n = 11$) mice. *I*: Mean energy intake ($\text{kcal} \cdot \text{day}^{-1} \cdot \text{mouse}^{-1}$) in control (CT; $n = 18$), LPS ($n = 18$), or high-fat diet-fed (HF; $n = 18$) mice. Data are means \pm SE. Data with different superscript letters are significantly different at $P < 0.05$, according to the post hoc ANOVA statistical analysis.

lence, blood glucose concentration was higher in LPS than in saline-treated mice (Fig. 2*B*). Similar data were obtained in 4-week high-fat diet-fed mice for the fasted and 15-min time points (Fig. 2*B*). However, the blood glucose concentration remained higher in the high-fat diet-fed mice compared with control and LPS-infused mice. The area under curves were higher in the LPS and high-fat diet-fed mice when compared with control mice (Fig. 2*B* inset). Furthermore, fasted insulinemia was higher in LPS- and high-fat-treated mice than in control mice. However, glucose-induced insulin secretion was normal in the chronic LPS-infused animals and was lower than control mice in high-fat diet-fed mice (Fig. 2*C*). Increased fasted plasma glucose and insulin levels were associated with liver but not with whole-body insulin resistance in chronic LPS-infused, whereas high-fat diet-fed mice were characterized with whole-body, but not liver, insulin resistance (Fig. 2*D*).

In addition, the 4-week LPS infusion increased body

weight to the same extent as a 4-week high-fat diet regimen (Fig. 2*E*). The visceral and subcutaneous adipose depots were similarly increased (Fig. 2*F*). This increase was more pronounced in the high-fat diet-fed mice. Liver weight was higher in the LPS-infused than in control and high-fat diet-fed mice (Fig. 2*G*). Liver triglyceride content was increased in both LPS-infused and high-fat diet-fed mice when compared with control mice, whereas significance was reached in the high-fat diet-fed group only (Fig. 2*H*). Energy intakes were quantified and found to be increased in the high-fat diet-fed group only when compared with control mice (Fig. 2*I*).

Metabolic endotoxemia triggers the expression of inflammatory factors similarly to high-fat diet: a CD14-dependent mechanism. We determined the expression pattern of the main inflammatory factors involved in metabolic diseases, after 2 and 4 weeks of a high-fat diet or subcutaneous chronic LPS infusion. The mRNA concentrations of TNF- α , IL-1, IL-6, and plasminogen activator

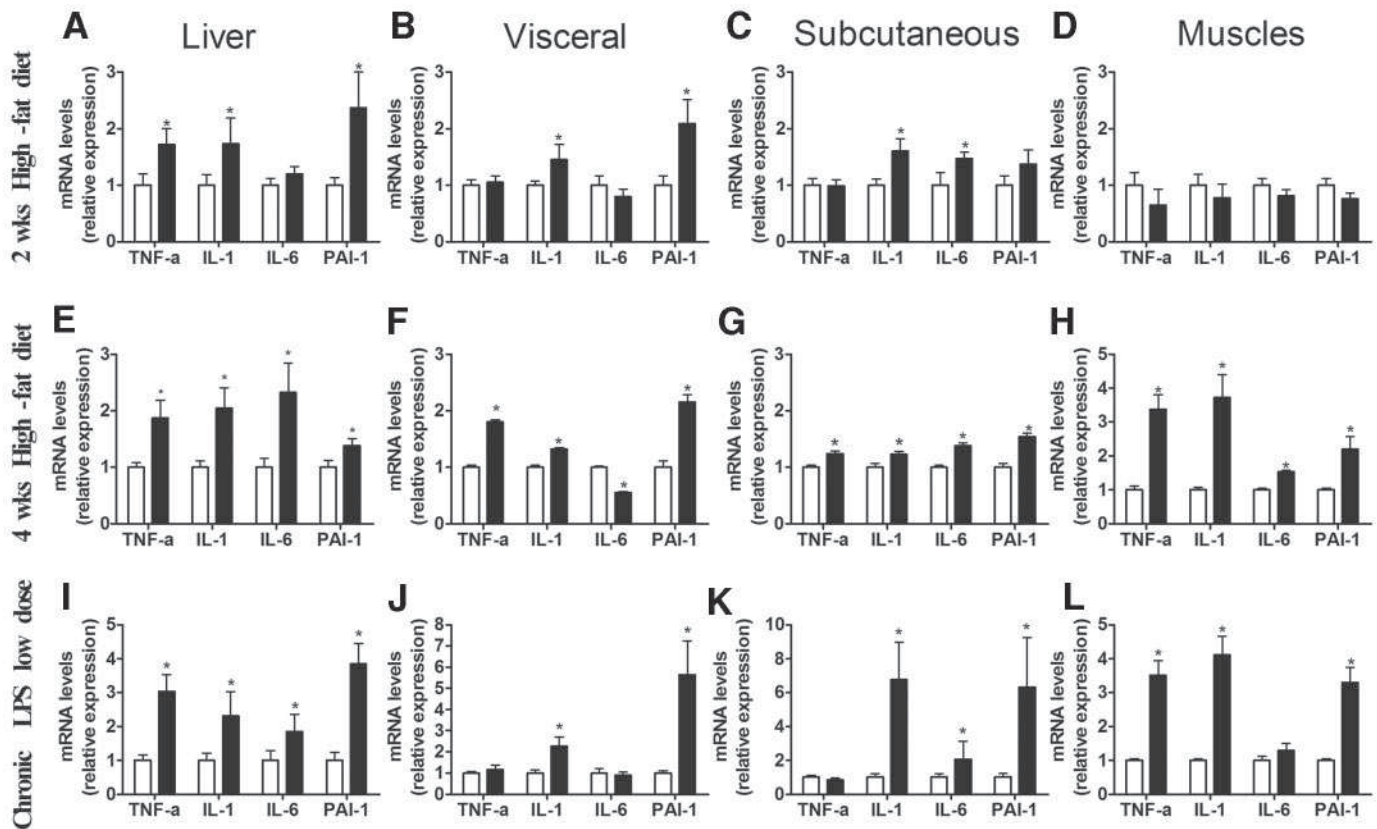


FIG. 3. Metabolic endotoxemia triggers the expression of inflammatory factors similarly to high-fat feeding. TNF- α , IL-1, IL-6, and PAI-1 mRNA concentrations (A, E, and I) in liver (B, F, and J), visceral adipose tissue (C, G, and K), subcutaneous adipose tissue (D, H, and L), and muscle in normal diet-fed ($n = 8$) (□) or high-fat diet-fed ($n = 8$) (■) mice for 2 weeks (A–D) and 4 weeks ($n = 8$) (E–H) and in LPS-infused mice ($n = 5$) (I–L). Data are means \pm SE. * $P < 0.05$ vs. normal chow-fed mice.

inhibitor (PAI)-1 were generally increased in various combinations in the liver, as well as in the visceral and subcutaneous depots, and in muscle of high-fat diet-fed and LPS-infused mice (Fig. 3). Interestingly, liver cytokines were increased as early as 2 weeks after commencement of the diet (Fig. 3A), which could also be related to the early augmentation of plasma LPS concentration (3.4 ± 0.3 EU/ml, compared with Fig. 2A). From these data, we can conclude that LPS mimics, to some extent, high-fat diet-induced inflammation and could be responsible for impaired metabolism.

To demonstrate the causal link between LPS and obesity/diabetes, we studied CD14 mutant mice. In wild-type (WT) mice, the acute 3-h intravenous LPS infusion markedly increased IL-6, PAI-1, and IL-1 mRNA concentrations in the subcutaneous adipose depot, whereas this increase was dramatically blunted in CD14 mutant mice (Figs. 4A and B). Furthermore, the concentration of phosphorylated nuclear factor- κ B and IKK forms were increased in the liver of WT mice and unchanged in CD14 mutant mice (Fig. 4C). We then quantified the effect of the chronic LPS infusion in WT and CD14 mutant mice. The data showed that body weight gain and visceral and subcutaneous adipose depot weights were increased in WT but unchanged in CD14 mutant mice (Figs. 5A and B). Furthermore, fasted and glucose-stimulated glycemia were augmented in WT-LPS-infused mice when compared with WT-CT mice (Fig. 5C). This observation was not apparent when CD14 mutant mice were infused with LPS. The area under the curve was increased in response to LPS infusion in the WT mice only (Fig. 5C, *inset*). Plasma insulin

concentrations were similar in the basal and glucose-stimulated conditions for all groups (Fig. 5D). Chronic LPS infusion increased liver weight in the WT mice only (Fig. 5E). Triglycerides were increased by 30% in the liver of LPS-infused WT mice but did not reach statistical significance when compared with all other conditions (Fig. 5F). All together, these data confirm that LPS is directly implicated in the alterations of body weight and glucose metabolism observed in Figs. 1 and 2 in the previous experiments.

CD14: the main LPS receptor sets the tone of insulin sensitivity and the occurrence of obesity and diabetes. We found that CD14 mutant mice are hypersensitive to insulin, as determined by the euglycemic-hyperinsulinemic clamp (Fig. 6A). These data show that CD14 itself can affect the basal physiological state of insulin sensitivity. Therefore, we challenged the mutant mice with a high-fat diet to delineate the relevance of hypersensitivity to insulin. We found that hypersensitivity to insulin allows the mutant mice to delay, without totally preventing, the occurrence of pathological insulin resistance and increased body weight (Fig. 6B) when fed a high-fat diet. Liver weight progressively increased and reached statistical significance after 24 weeks of a high-fat diet in WT mice (Fig. 6C). This increase was prevented in CD14 mutant mice. Similarly, liver triglyceride concentration was increased after only 4 weeks of a high-fat regimen (Fig. 6D). This was totally blunted in the CD14 mutant mice. Similarly, oil red O staining showed that lipid accumulation was blunted in the CD14 mutant fed a high-fat diet or infused with LPS (Fig. 6E). WT and CD14

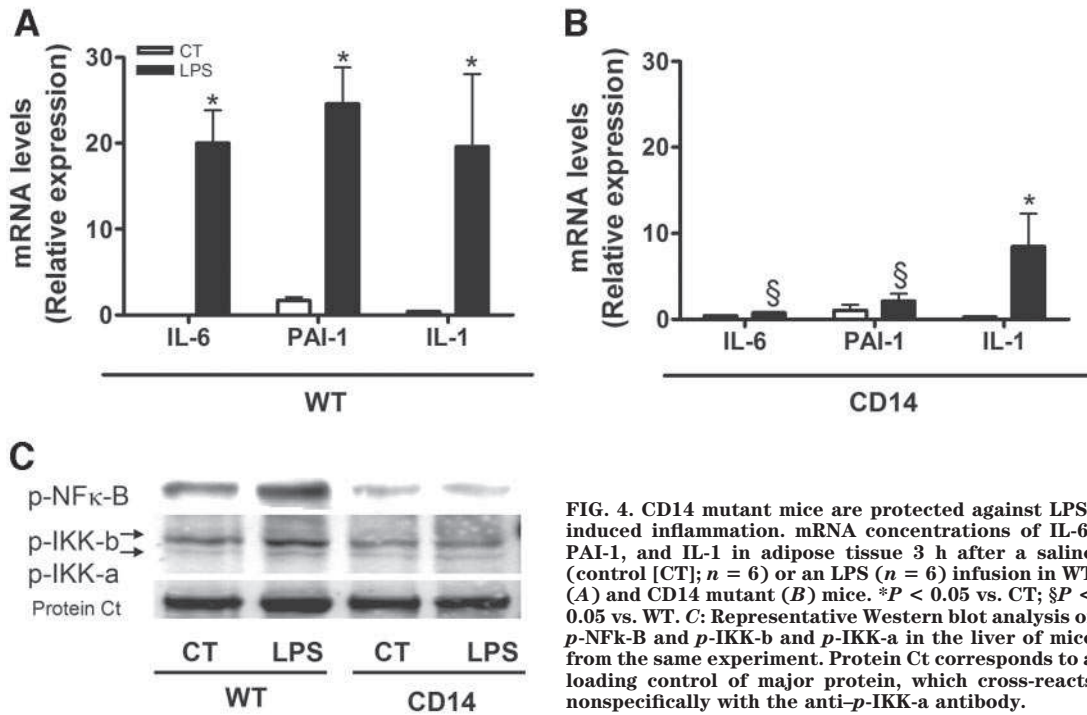


FIG. 4. CD14 mutant mice are protected against LPS-induced inflammation. mRNA concentrations of IL-6, PAI-1, and IL-1 in adipose tissue 3 h after a saline [CT; $n = 6$] or an LPS ($n = 6$) infusion in WT (A) and CD14 mutant (B) mice. * $P < 0.05$ vs. CT; § $P < 0.05$ vs. WT. C: Representative Western blot analysis of p-NFκ-B and p-IKK-b and p-IKK-a in the liver of mice from the same experiment. Protein Ct corresponds to a loading control of major protein, which cross-reacts nonspecifically with the anti-p-IKK-a antibody.

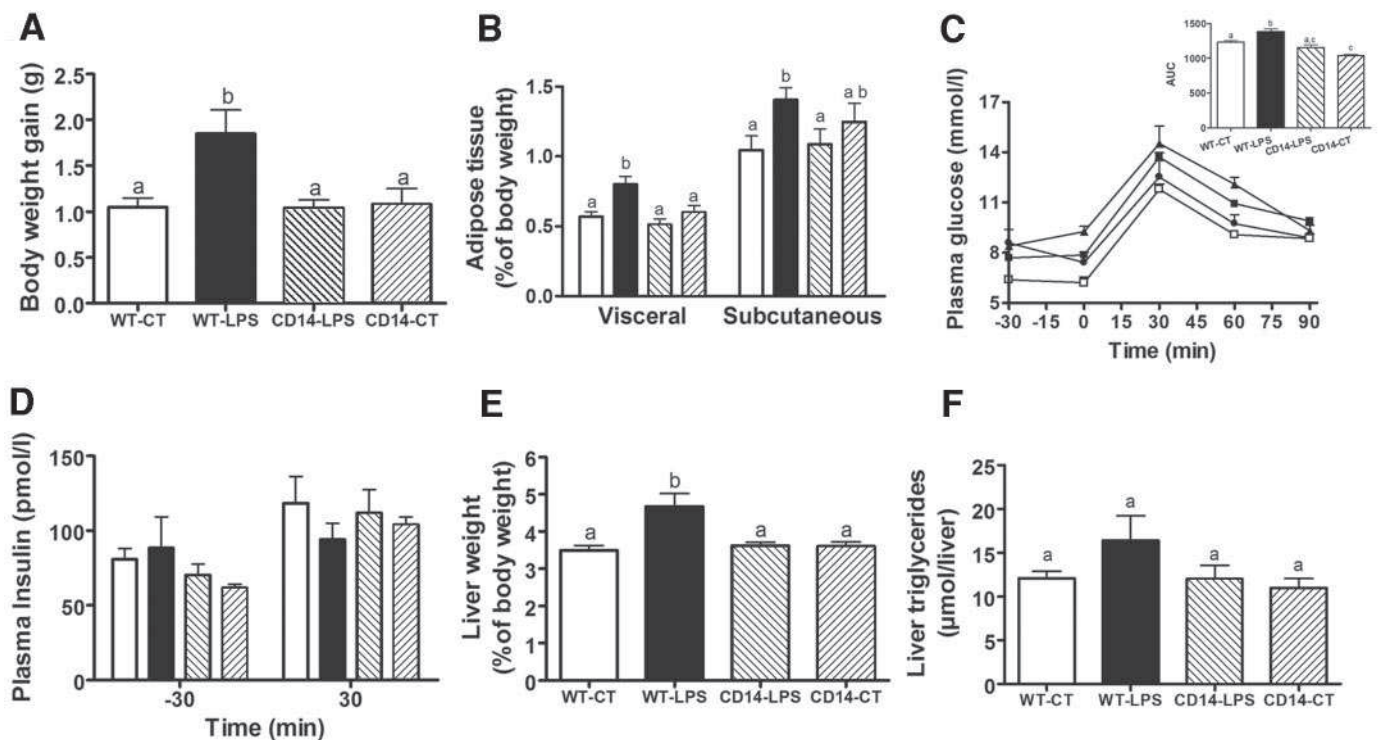


FIG. 5. The CD14 null mutation prevents the effect of LPS-induced obesity and diabetes. A: Body weight gain (g) in WT mice infused with saline (WT-CT; $n = 13$) or LPS (WT-LPS; $n = 14$) and CD14 mutant mice infused with saline (CD14-CT; $n = 13$) or LPS (CD14-LPS; $n = 12$) for 4 weeks using subcutaneous osmotic pumps. B: Visceral and subcutaneous adipose tissue weight (percentage of body weight) in WT-CT ($n = 13$) (□), WT-LPS ($n = 14$) (■), CD14-CT ($n = 13$) (▨), and CD14-LPS ($n = 12$) (▩) mice. C: Plasma glucose concentration (mmol/l) following an intraperitoneal glucose load (1 g/kg) in WT-CT ($n = 6$) (□), WT-LPS ($n = 6$) (■), CD14-CT ($n = 5$) (▨), and CD14-LPS ($n = 6$) (●) mice. The inset represents the area under curve of the same groups. D: Plasma insulin (pmol/l) concentration 30 min before (-30) and 30 min after (30) intraperitoneal glucose administration in WT-CT ($n = 6$) (□), WT-LPS ($n = 6$) (■), CD14-CT ($n = 5$) (▨), and CD14-LPS ($n = 6$) (▩) mice. E: Liver weight (percentage of body weight) in WT-CT ($n = 13$), WT-LPS ($n = 13$), CD14-CT ($n = 12$), and CD14-LPS ($n = 13$) mice. F: Liver triglycerides (μmol/liver) in WT-CT ($n = 12$), WT-LPS ($n = 9$), CD14-CT ($n = 5$), and CD14-LPS ($n = 6$) mice. Data are means ± SE. Data with different superscript letters are significantly different at $P < 0.05$, according to the post hoc ANOVA statistical analysis.

mutant mice both became glucose intolerant after 24 weeks of high-fat diet (Fig. 6F). In addition, WT high-fat diet-fed (WT-HF) but not CD14 mice became hyperinsulinemic after 24 weeks of a high-fat diet (Fig. 6G).

We performed a closer analysis of these mice after 4 weeks of a high-fat diet, when insulin resistance is already present in WT but not in CD14 mutant mice. After only 4 weeks of high-fat diet, the CD14 mutant mice had normal fasted glycemia, remained normally tolerant to glucose (Fig. 7A), and did not become hyperinsulinemic (Fig. 7B) in the fasting state when compared with WT mice. Visceral adipose depot weight was increased in WT but not in CD14 mutant mice fed a high-fat diet (Fig. 7C), whereas subcutaneous adipose depot was increased in both genotypes during high-fat diet (Fig. 7C). Furthermore, TNF- α and PAI-1 mRNA concentrations were both increased by the high-fat diet in WT mice, whereas this increase was totally blunted in the CD14 mutant mice (Fig. 7D). In the liver, a similar tendency was observed as in the adipose depot, showing that in absence of CD14 a high-fat diet could not induce inflammation (Fig. 7E). Although, PAI-1 mRNA levels are significantly elevated in CD14 high-fat-fed mice relative to controls.

CD14 mutant mice resist high-fat diet-induced adipose depot macrophages infiltration and partly reduce adipocyte hypertrophy. Adipose cell size was increased in WT-HF mice when compared with WT-CT mice and to a lower extent in CD14 mutant mice (Figs. 8A, C, and D). Conversely, the mean adipocyte size was reduced in WT-LPS infused but not in CD14 mutant mice (Figs. 8B–D). These changes in adipocyte size were accompanied with variations in F4/80-positive cells present in the subcutaneous adipose depots (Fig. 8E). High-fat feeding and LPS increased the number of F4/80-positive cells in WT mice. This was totally abolished in CD14 mutant mice (Fig. 8E).

DISCUSSION

We report here for the first time that high-fat feeding augments plasma LPS at a concentration sufficient to increase body weight, fasted glycemia, and inflammation. LPS infusion in normal diet-fed mice causes a metabolic response similar, to some extent, to high-fat feeding. LPS receptor-deleted mice (i.e., CD14 mutants) are hypersensitive to insulin, and the occurrence of insulin resistance, obesity, and diabetes is delayed in response to high-fat feeding. Hence, we conclude that the LPS/CD14 system sets the threshold at which high-fat diet-induced metabolic disease occurs.

Central to metabolic diseases is insulin resistance associated with a low-grade inflammatory status. In our quest to determine a triggering factor of the early development of metabolic disease, we looked for a molecule involved early in the cascade of inflammation and identified LPS as a good candidate. Furthermore, LPS is a strong stimulatory of the release of several cytokines that are key inducers of insulin resistance. The concept of dietary excess is essentially linked to high-fat feeding-induced inflammation (24). As we identified here, LPS as a putative factor for the triggering of metabolic diseases. We needed to challenge our hypothesis within a pathological context. We fed mice a high-fat diet for a short period of 2–4 weeks and showed that high-fat diet increases the circulating concentration of plasma LPS. Hence, we defined this increase in plasma LPS concentration induced by high-fat feeding as metabolic endotoxemia. It is noteworthy that

the endotoxemia reached was 10–50 times lower than that obtained during septic shock (22,25). The mechanisms allowing enteric LPS absorption are unclear but could be related to an increased filtration of plasma LPS into lymph with fat absorption (26). Endogenous LPS is continually produced within the gut by the death of Gram-negative bacteria (27) and is absorbed into intestinal capillaries (28,29) to be transported by lipoproteins (14,15). Therefore, we assessed whether a high-fat diet changed intestinal microbiota and showed that among the dominant members of the intestine the Gram-negative *Bacteroides*-related bacteria MIB were significantly reduced in the high-fat diet-fed animals compared with control animals. However, numbers of the dominant Gram-positive group, the *Eu. rectale-Cl. coccoides* group, were also reduced, as were numbers of bifidobacteria, a group of bacteria that have been shown to reduce intestinal endotoxin (LPS) levels in mice and improve mucosal barrier function (30,31). Supporting our conclusion, apart from further evidence from the literature, was the result that an acute ingestion of LPS, diluted in oil, reproduced high-fat diet-increased plasma LPS concentration. Furthermore, oil by itself can acutely increase endotoxemia. We could therefore suggest that plasma LPS levels depends on feeding status and are physiologically regulated nutrients. We challenged this hypothesis in mice assessing endotoxemia throughout the day and showed that plasma LPS concentration increases progressively over the feeding period (night in the mouse). As the daily endotoxemia cycle was totally disrupted during high-fat feeding, our data showed that the fat content in food is an important regulator of plasma LPS concentration. In light of the changes observed in the microbiota of high-fat diet-fed mice, one could suggest that an increased continuous intestinal absorption of LPS could maintain steady and elevated the endotoxemia. Such a conclusion is also supported by our epidemiological study in humans in which healthy patients feeding on a fat-enriched diet were characterized by a higher fasting endotoxemia (data not shown).

To assess whether a two- to three-times-increased daily endotoxemia could be considered as a physiological regulator, glucose metabolism was assessed in mice in which we continuously infused a very low rate of LPS. We found that the body and adipose depot weights and fasted glycemia were increased to the same extent as during high-fat feeding. Furthermore, the chronic LPS infusion induced liver insulin resistance and was associated with fasted hyperinsulinemia. As whole-body insulin resistance was not induced by the LPS infusion, our data showed the liver as a first target of LPS-induced insulin resistance. The role of LPS as a regulator of energy metabolism has been proposed previously (32,33). In most of the studies that described the anorectic and metabolic effects of LPS, endotoxemia was very elevated or given as single shot and witnessed a state of acute phase infection. Here, we showed that the chronic infusion of a very low rate of LPS increased body weight. However, this increase was not due to an excessive energy intake.

We then studied the CD14 mutant mice, in which the expression of the protein is suppressed by a point mutation (34). CD14 is a key molecule in innate immunity (35). It is a multifunctional receptor phosphatidylinositol phosphate-anchored glycoprotein of 55 kDa constitutively expressed in considerable amounts on the surface (mCD14) of mature monocytes, macrophages, and neutrophils (36,37). The binding of LPS to the complex of mCD14

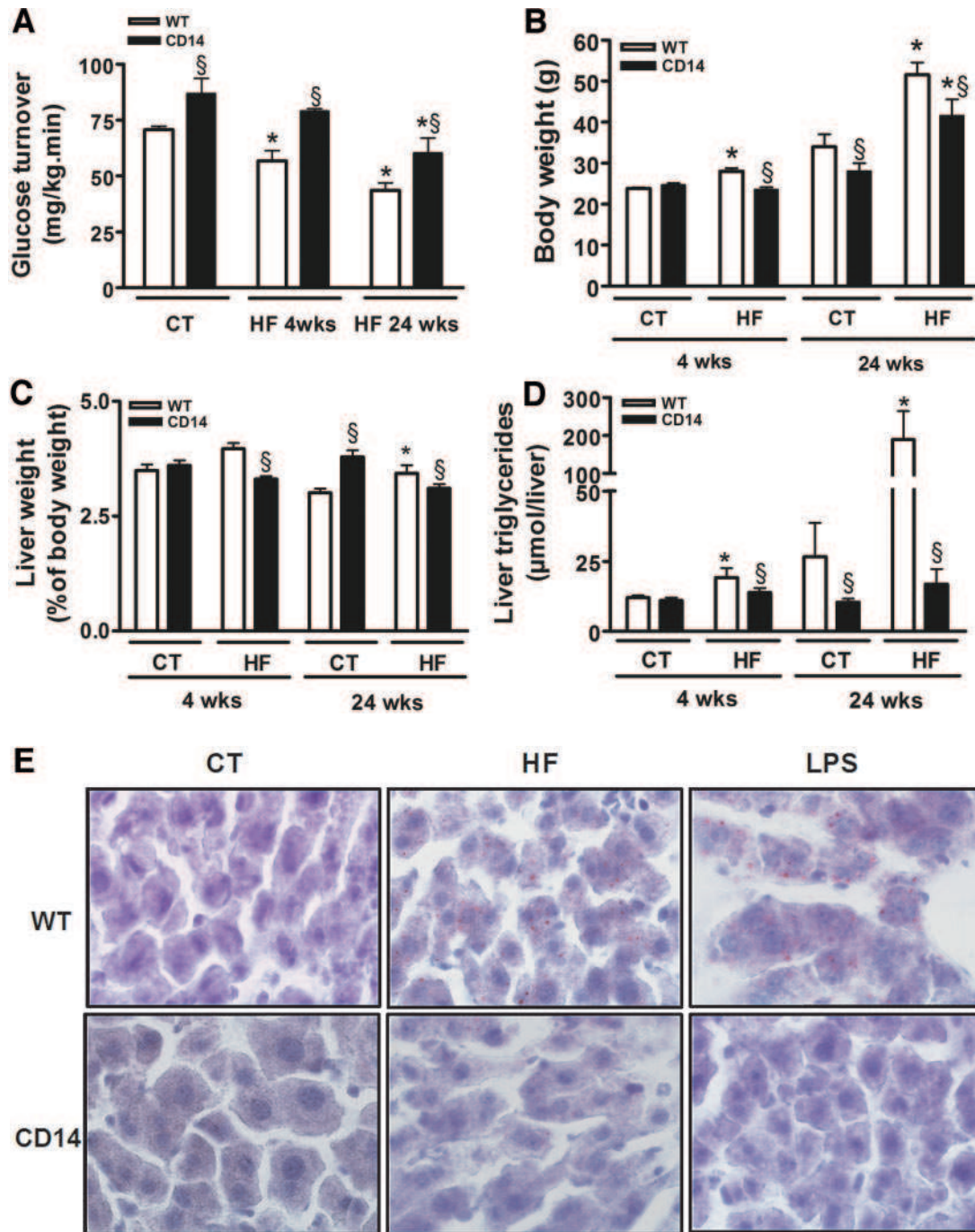


FIG. 6. CD14: the main LPS receptor sets the tone of insulin sensitivity and hepatic steatosis. **A:** Glucose turnover ($\text{mg} \cdot \text{kg}^{-1} \cdot \text{min}^{-1}$) in WT mice or CD14 mutant fed a normal diet (CT) or fed a high-fat diet (HF) for 4 ($n = 8$) or 24 ($n = 8$) weeks (wks). **B:** Body weight gain (g) in WT or CD14 mutant fed a normal diet (CT) for 4 ($n = 8$) or 24 ($n = 8$) weeks or fed a high-fat diet (HF) for 4 ($n = 8$) or 24 ($n = 8$) weeks. **C:** Liver weight (percent of body weight) in WT or CD14 mutant mice fed a normal diet (CT) for 4 ($n = 8$) or 24 ($n = 8$) weeks or fed a high-fat diet (HF) for 4 ($n = 8$) or 24 ($n = 8$) weeks. **D:** Liver triglycerides ($\mu\text{mol/liver}$) in WT or CD14 mutant mice fed a normal diet (CT) for 4 ($n = 6$) or 24 ($n = 5$) weeks or fed a high-fat diet (HF) for 4 ($n = 5$) or 24 ($n = 5$) weeks. Data are means \pm SE. * $P < 0.05$ vs. CT; § $P < 0.05$ vs. WT. **E:** Representative oil red O liver staining in 4-week-treated mice. **F** (see next page): Plasma glucose following an intraperitoneal glucose load (1 g/kg) in WT mice fed a normal diet (WT-CT; $n = 8$) or a high-fat diet (WT-HF; $n = 8$) for 24 weeks and CD14 mutant mice fed a normal diet (CD14-CT; $n = 8$) or fed a high-fat diet (CD14-HF; $n = 8$). The inset represents the area under curve of the same groups. **G** (see next page): Fasting plasma insulin (pmol/l) in WT or CD14 mutant mice fed a normal diet (CT) for 4 ($n = 6$) or 24 ($n = 5$) weeks or fed a high-fat diet (HF) for 4 ($n = 5$) or 24 ($n = 5$) weeks. Data are means \pm SE. * $P < 0.05$ vs. CT; § $P < 0.05$ vs. WT. Data with different superscript letters are significantly different at $P < 0.05$, according to the post hoc ANOVA statistical analysis.

and TLR4 at the surface of the innate immune cells (15) triggers the secretion of proinflammatory cytokines (16), consequently affecting insulin action. Mice depleted of the CD14 gene lack the innate immune response to bacterial LPS, and CD14-deficient macrophages do not secrete

proinflammatory cytokines when stimulated with LPS (38). We have shown here that CD14 mutant mice fed a normal diet were hypersensitive to insulin. Therefore, CD14 could clearly be an early modulator of insulin sensitivity and, indeed, when challenged by a high-fat diet

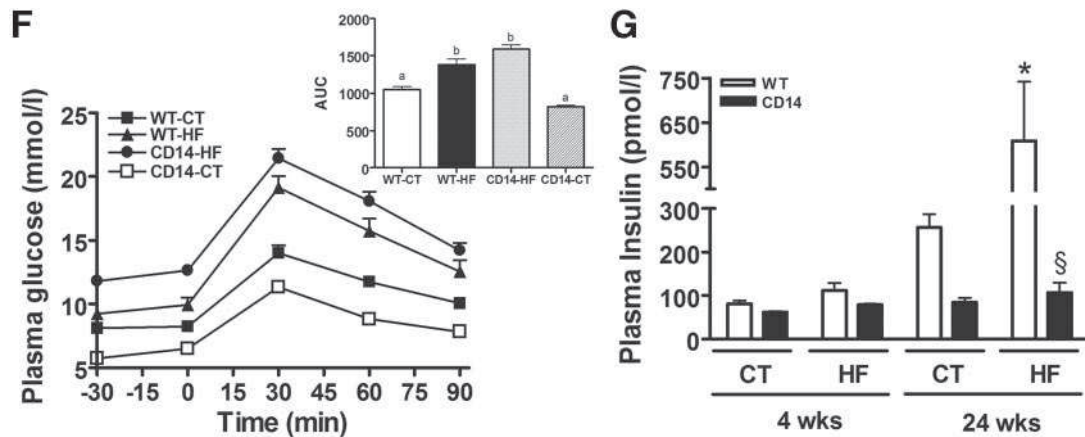


FIG. 6—Continued

for 1 month the insulin-hypersensitive CD14 mutant mice did not become insulin resistant, glucose intolerant, or diabetic. However, after long-term feeding (24 weeks), the CD14 mutant mice did become insulin resistant and gained weight. Furthermore, hepatic steatosis, as reflected by the triglyceride content, was totally prevented in CD14 mutants during long-term high-fat feeding. Hepatic steatosis is an early event because only 4 weeks of high-fat feeding were sufficient to increase the triglyceride content of wild-type mice. This could be mimicked by a 4-week LPS infusion. Again, hepatic steatosis was totally blunted in CD14 mutant fed a high-fat diet or infused with LPS. We

could conclude that the LPS-CD14 system sets a threshold at which metabolic diseases occur. Moreover, and relevant to our findings, epidemiological data from the literature showed statistical relationships between CD14 (39,40) inflammation, obesity, and insulin resistance in humans.

LPS-treated mice developed inflammation, as the expression of genes coding for cytokines, IL-6, TNF- α , IL-1, and PAI-1 were increased in adipose depots, liver, and muscle. Importantly, these features occurred similarly in high-fat diet-fed mice. Interestingly, liver cytokines were increased as early as after 2 weeks of high-fat feeding, suggesting that the liver was most likely the first organ

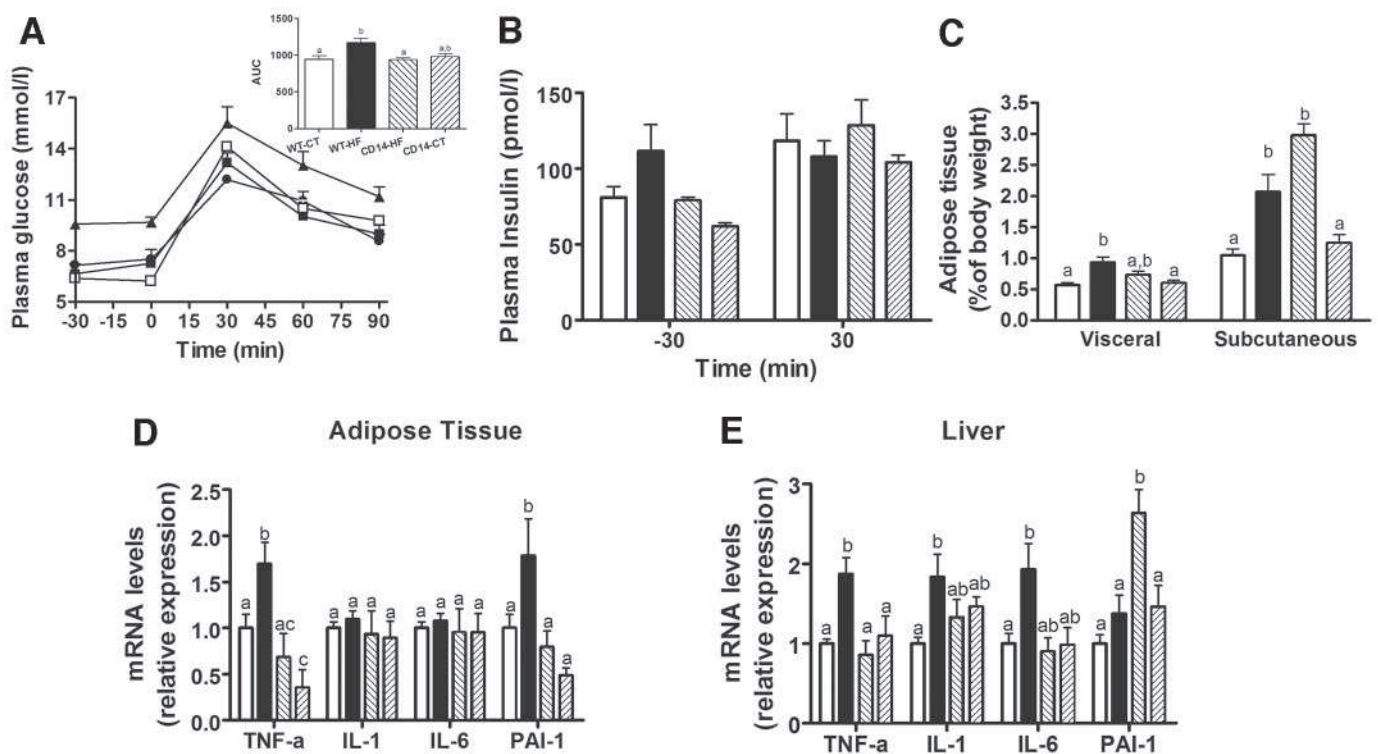


FIG. 7. CD14 mutant mice resist high-fat diet-induced glucose intolerance, inflammation, and increased visceral fat mass. **A:** Plasma glucose (mmol/l) following an intraperitoneal glucose load (1 g/kg) in WT mice fed a normal diet (WT-CT; $n = 6$) (■) or a high-fat diet (WT-HF; $n = 6$) (▲) for 4 weeks and CD14 mutant mice fed a normal diet (CD14-CT; $n = 5$) (●) or fed a high-fat diet (CD14-HF; $n = 5$) (□). The inset represents the area under curve of the same groups. **B:** Plasma insulin concentration (pmol/l) 30 min before (−30) and 30 min after (30) intraperitoneal glucose administration in WT-CT ($n = 6$) (□), WT-HF ($n = 6$) (■), CD14-CT ($n = 5$) (▨), and CD14-HF ($n = 5$) (▩) mice. **C:** Visceral and subcutaneous adipose tissue weight (percent of body weight) in WT-CT ($n = 6$) (□), WT-HF ($n = 6$) (■), CD14-CT ($n = 5$) (▨), and CD14-HF ($n = 5$) (▩) mice. **D:** Adipose tissue mRNA levels of TNF- α , IL-1, IL-6, and PAI-1 in WT-CT ($n = 6$) (□), WT-HF ($n = 6$) (■), CD14-CT ($n = 5$) (▨), and CD14-HF ($n = 5$) (▩) mice. **E:** Liver mRNA levels of TNF- α , IL-1, IL-6, and PAI-1 in WT-CT ($n = 6$) (□), WT-HF ($n = 6$) (■), CD14-CT ($n = 5$) (▨), and CD14-HF ($n = 5$) (▩) mice. Data are means \pm SE. Data with different superscript letters are significantly different at $P < 0.05$, according to the post hoc ANOVA statistical analysis.

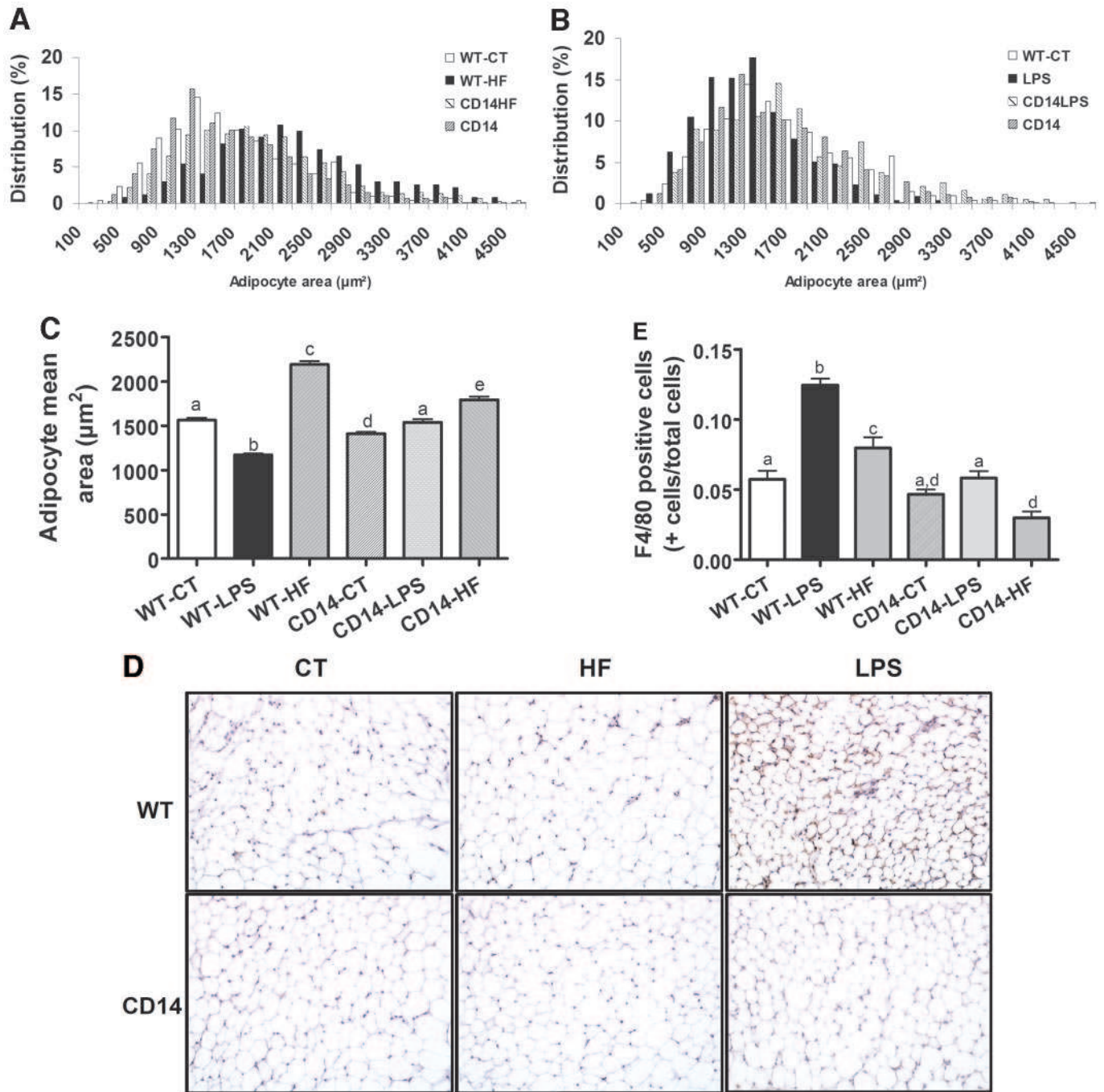


FIG. 8. Metabolic endotoxemia impairs adipocyte morphology. **A:** Adipocyte size distribution (%) in WT mice fed a normal diet (WT-CT; $n = 765$) (□) or a high-fat diet (WT-HF; $n = 661$) (■) for 4 weeks or CD14 mutant mice fed a normal diet (CD14-CT; $n = 1,032$) (▨) or a high-fat diet (CD14-HF; $n = 729$) (▩) for 4 weeks. **B:** Adipocyte size distribution (%) in WT mice infused with saline (WT-CT; $n = 765$) (□) or LPS (WT-LPS; $n = 750$) (■) and CD14 mutant mice infused with saline (CD14-CT; $n = 1,032$) (▨) or LPS (CD14-LPS; $n = 585$) (▩) for 4 weeks using subcutaneous osmotic pumps. **C:** Adipocyte mean area (μm^2) in WT-CT ($n = 765$), WT-HF ($n = 661$), WT-LPS ($n = 750$), CD14-CT ($n = 1,032$), CD14-HF ($n = 729$), or CD14-LPS ($n = 585$) mice. **D:** Representative adipose tissue staining in 4-week-treated mice. **E:** F4/80-positive cells (+ cells/total cells) of all above groups. Data are means \pm SE. Data with different superscript letters are significantly different at $P < 0.05$, according to the post hoc ANOVA statistical analysis.

affected by LPS treatment. Evidence from the literature supports our hypothesis. It has been shown that LPS is a strong inducer of nonalcoholic hepatic steatosis (41), another feature related to metabolic diseases. In addition, genetically obese *fa/fa* rats and *ob/ob* mice quickly develop steatohepatitis after exposure to low doses of LPS (41). This is in agreement with a two- to four-times-increased endotoxemia characterizing *db/db* and *ob/ob* mice due to

an increased intestinal permeability (42). Furthermore, polymyxin B treatment, which specifically eliminates Gram-negative bacterias and further quenches LPS, diminishes hepatic steatosis (43). Our data demonstrate that in absence of CD14, a high-fat diet could not induce inflammation as reflected by the total blunting of cytokine expression augmentation in the liver and adipose depot. Similarly, we recently reported that TLR4 mutant mice are

protected against adipose tissue insulin resistance (44). Our finding is complementary to recent data that showed that free fatty acids can bind TLR4 to activate cells from the innate immune system (6) leading to the secretion of cytokines. This was totally blunted in TLR4 mutant mice. Therefore, our data suggest that TLR4 requires CD14, as a rate-limiting step, to mediate lipid-induced cytokine secretion because in the absence of CD14 high-fat diet could not induce inflammation *in vivo*; therefore, TLR4 is not sufficient. Another difference between the TLR4 and CD14 mutant mice is that the former became obese and hyperphagic, whereas CD14 mice delay the occurrence of obesity and showed no change in feeding behavior.

Furthermore, whereas macrophage infiltration was increased in adipose tissue of wild-type mice fed a high-fat diet and in mice infused with LPS, this effect was totally blunted in absence of CD14. The mechanism involved in the recruitment of macrophages in the adipose depot seems to be different from the LPS coreceptor TLR4, as the corresponding mutant mice were still characterized by a high adipose tissue macrophage infiltration in response to high-fat diet (7,45). Conversely, TLR4 overexpression led to some extent of adipose insulin resistance (8). An original observation from our present work was that LPS increased the number of subcutaneous adipocytes of a smaller size. This is opposite to what observed in high-fat diet-fed mice. Again, CD14 mutant mice resist, to some extent, the changes in adipocyte size and number in response to high fat and LPS.

The origin of metabolic diseases due to high-fat-induced metabolic endotoxemia is unclear but could be related to the microbiota present in the digestive tract. Recently, an original observation reported that young adult mice have 40% more total body fat than their germ-free counterpart fed the same diet (10,46). Similarly, lean axenic mice colonized with microbiota from *ob/ob* mice increased body weight. The authors suggested that gut microbiota from obese mice allows energy to be salvaged from otherwise-indigestible dietary polysaccharides. This hypothesis was further demonstrated by the fact that colonization increases glucose uptake in the host intestine and produces substantial elevations in serum glucose and insulin, both factors being lipogenic. However, this hypothesis of microbiota-induced lipogenesis could not explain either the inflammatory dimension of the mechanism linking dietary excess to obesity/diabetes or the differential effect on body weight of a high-fat diet versus a regular diet. However, axenic mice fed a high-fat obesitogenic diet did not gain weight, suggesting that, indeed, a bacterially related factor is responsible for high-fat diet-induced obesity (11). We suggest that LPS would be such a permissive factor that, upon binding to CD14, could lead to obesity. Therefore, lipids alone are not sufficient to promote obesity. Another recent report (12) showed that antibiotic treatment protected against the occurrence of autoimmune diabetes. The authors suggest that the gut microbiota generates inflammation and makes the rats prone to becoming diabetic. Hence, our data strongly support that metabolic endotoxemia would mediate the well-characterized low-tone inflammatory status of the metabolic disease. We suggest that LPS would be a newly identified inflammatory factor from microbiota, which upon binding to CD14 serves as vector for the triggering of obesity/insulin resistance induced by high-fat feeding. Along the same line of investigation, we previously reported that reducing the Gram-negative bacterial content of the digestive track by

the mean of dietary fibers was also associated with reduced body weight (17,47).

In conclusion, we demonstrate first that metabolic concentrations of plasma LPS are modulated by fat food content. Second, we found that metabolic concentrations of plasma LPS are a sufficient molecular mechanism for triggering the high-fat diet-induced metabolic diseases obesity/diabetes. Finally, the LPS receptor CD14, by controlling insulin sensitivity, sets the threshold at which metabolic diseases occur.

ACKNOWLEDGMENTS

P.D.C. is a Postdoctoral Researcher from the FNRS (Fonds de la Recherche Scientifique), Belgium. R.B. is the recipient of subsidies from the Nutritia Foundation, the AFERO (Association Française Etude et de Recherche sur les Obésités), the FRM (Fondation pour la Recherche Médicale), the ATIP (Action Thématiques Incitatives sur Programme), and the ACI (Action Concertée Incitative), Centre de la Recherche Nationale Scientifique, Université Paul Sabatier. J.A. is a recipient of a grant from the SFHTA (Société Française d'Hypertension Artérielle) and the délégation régionale à la recherche clinique des hôpitaux de Toulouse (in 2003). This work also was supported by the Programme National de Recherche sur les Maladies Cardiovasculaires, INSERM: "Vascular Risk and Metabolic Syndrome: Hemostasis, Inflammation and Metabolism Interplay" (no. A04046AS) (to M.C.A.). This work was supported by a Fonds Speciaux de Recherche grant from the Université catholique de Louvain and FNRS grant to N.M.D.

We thank Drs. B. Pipy, J.F. Arnal, C. Feyt, and P. Gourdy for helpful criticisms and N. Maton and C. Dray for excellent technical assistance.

REFERENCES

- Magnan C, Collins S, Berthault M, Kassis N, Vincent M, Gilbert M, Penicaud L, Ktorza A, Assimakopoulos-Jeannet F: Lipid infusion lowers sympathetic nervous activity and leads to increased beta-cell responsiveness to glucose. *J Clin Invest* 103:413–419, 1999
- Wellen KE, Hotamisligil GS: Inflammation, stress, and diabetes. *J Clin Invest* 115:1111–1119, 2005
- Hotamisligil GS, Shargill NS, Spiegelman BM: Adipose expression of tumor necrosis factor- α : direct role in obesity-linked insulin resistance. *Science* 259:87–91, 1993
- Weisberg SP, McCann D, Desai M, Rosenbaum M, Leibel RL, Ferrante AW Jr: Obesity is associated with macrophage accumulation in adipose tissue. *J Clin Invest* 112:1796–1808, 2003
- Hotamisligil G, Peraldi P, Budavari A, Ellis R, White M, Spiegelman B: IRS-1-mediated inhibition of insulin receptor tyrosine kinase activity in TNF- α -and obesity-induced insulin resistance. *Science* 271:665–668, 1996
- Shi H, Kokoeva MV, Inouye K, Tzameli I, Yin H, Flier JS: TLR4 links innate immunity and fatty acid-induced insulin resistance. *J Clin Invest* 116:3015–3025, 2006
- Suganami T, Mieda T, Itoh M, Shimoda Y, Kamei Y, Ogawa Y: Attenuation of obesity-induced adipose tissue inflammation in C3H/HeJ mice carrying a Toll-like receptor 4 mutation. *Biochem Biophys Res Commun* 354:45–49, 2007
- Song MJ, Kim KH, Yoon JM, Kim JB: Activation of toll-like receptor 4 is associated with insulin resistance in adipocytes. *Biochem Biophys Res Commun* 346:739–745, 2006
- Ley RE, Backhed F, Turnbaugh P, Lozupone CA, Knight RD, Gordon JI: Obesity alters gut microbial ecology. *Proc Natl Acad Sci U S A* 102:11070–11075, 2005
- Backhed F, Ding H, Wang T, Hooper LV, Koh GY, Nagy A, Semenkovich CF, Gordon JI: The gut microbiota as an environmental factor that regulates fat storage. *Proc Natl Acad Sci U S A* 101:15718–15723, 2004
- Backhed F, Manchester JK, Semenkovich CF, Gordon JI: Mechanisms

- underlying the resistance to diet-induced obesity in germ-free mice. *Proc Natl Acad Sci U S A* 104:979–984, 2007
12. Brugman S, Klatte FA, Visser JT, Wildeboer-Veloo AC, Harmsen HJ, Rozing J, Bos NA: Antibiotic treatment partially protects against type 1 diabetes in the bio-breeding diabetes-prone rat: is the gut flora involved in the development of type 1 diabetes? *Diabetologia* 49:2105–2108, 2006
 13. Neal MD, Leaphart C, Levy R, Prince J, Billiar TR, Watkins S, Li J, Cetin S, Ford H, Schreiber A, Hackam DJ: Enterocyte TLR4 mediates phagocytosis and translocation of bacteria across the intestinal barrier. *J Immunol* 176:3070–3079, 2006
 14. Vreugdenhil AC, Rousseau CH, Hartung T, Greve JW, van 't Veer C, Buurman WA: Lipopolysaccharide (LPS)-binding protein mediates LPS detoxification by chylomicrons. *J Immunol* 170:1399–1405, 2003
 15. Wright SD, Ramos RA, Tobias PS, Ulevitch RJ, Mathison JC: CD14, a receptor for complexes of lipopolysaccharide (LPS) and LPS binding protein. *Science* 249:1431–1433, 1990
 16. Sweet MJ, Hume DA: Endotoxin signal transduction in macrophages. *J Leukoc Biol* 60:8–26, 1996
 17. Knauf PD, Knauf C, Iglesias M, Drucker D, Delzenne N, Burcelin R: Improvement of glucose tolerance and hepatic insulin sensitivity by oligofructose requires a functional GLP-1 receptor. *Diabetes* 55:1484–1490, 2006
 18. Knauf C, Cani PD, Perrin C, Iglesias M, Maury J, Bernard E, Benhamed F, Grémeaux T, Drucker D, Kahn C, Girard J, Tanti J, Delzenne N, Postic C, Burcelin R: Brain glucagon-like peptide-1 increases insulin secretion and muscle insulin resistance to favor hepatic glycogen storage. *J Clin Invest* 115:3554–3563, 2005
 19. Burcelin R, Uldry M, Foretz M, Perrin C, Dacosta A, Nenniger-Tosato M, Seydoux J, Cotecchia S, Thorens B: Impaired glucose homeostasis in mice lacking the alpha β -adrenergic receptor subtype. *J Biol Chem* 279:1108–1115, 2004
 20. Tuohy KM, Kolida S, Lustenberger AM, Gibson GR: The prebiotic effects of biscuits containing partially hydrolyzed guar gum and fructo-oligosaccharides: a human volunteer study. *Br J Nutr* 86:341–348, 2001
 21. Knauf C, Rieusset J, Foretz M, Cani PD, Uldry M, Hosokawa M, Martinez E, Bringart M, Waget A, Kersten S, Desvergne B, Grenlich S, Wahli W, Seydoux J, Delzenne NM, Thorens B, Burcelin R: Peroxisome proliferator-activated receptor- α -null mice have increased white adipose tissue glucose utilization, GLUT4, and fat mass: role in liver and brain. *Endocrinology* 147:4067–4078, 2006
 22. Mydel P, Takahashi Y, Yumoto H, Sztukowska M, Kubica M, Gibson FC 3rd, Kurtz DM Jr, Travis J, Collins LV, Nguyen KA, Genco CA, Potempa J: Roles of the host oxidative immune response and bacterial antioxidant rubrerythrin during *Porphyromonas gingivalis* infection. *PLoS Pathog* 2:e76, 2006
 23. Salzman NH, de Jong H, Paterson Y, Harmsen HJ, Welling GW, Bos NA: Analysis of 16S libraries of mouse gastrointestinal microflora reveals a large new group of mouse intestinal bacteria. *Microbiology* 148:3651–3660, 2002
 24. Corcos M, Guilbaud O, Paterniti S, Moussa M, Chambry J, Chaouat G, Consoli S, Jeammet P: Involvement of cytokines in eating disorders: a critical review of the human literature. *Psychoneuroendocrinology* 28:229–249, 2003
 25. Mitaka C: Clinical laboratory differentiation of infectious versus non-infectious systemic inflammatory response syndrome. *Clin Chim Acta* 351:17–29, 2005
 26. Black DD, Tso P, Weidman S, Sabesin SM: Intestinal lipoproteins in the rat with D-(+)-galactosamine hepatitis. *J Lipid Res* 24:977–992, 1983
 27. Drewe J, Beglinger C, Fricker G: Effect of ischemia on intestinal permeability of lipopolysaccharides. *Eur J Clin Invest* 31:138–144, 2001
 28. Moore F, Moore E, Poggetti R, McAnena O, Peterson V, Abernathy C: Gut bacterial translocation via the portal vein: a clinical perspective with major torso trauma. *J Trauma* 31:629–636, 1991
 29. Tomita M, Ohkubo R, Hayashi M: Lipopolysaccharide transport system across colonic epithelial cells in normal and infective rat. *Drug Metab Pharmacokin* 19:33–40, 2004
 30. Griffiths EA, Duffy LC, Schanbacher FL, Qiao H, Dryja D, Leavens A, Rossman J, Rich G, Dirienzo D, Ogra PL: In vivo effects of bifidobacteria and lactoferrin on gut endotoxin concentration and mucosal immunity in Balb/c mice. *Dig Dis Sci* 49:579–589, 2004
 31. Wang Z, Xiao G, Yao Y, Guo S, Lu K, Sheng Z: The role of bifidobacteria in gut barrier function after thermal injury in rats. *J Trauma* 61:650–657, 2006
 32. Steiger M, Senn M, Altreuther G, Werling D, Sutter F, Kreuzer M, Langhans W: Effect of a prolonged low-dose lipopolysaccharide infusion on feed intake and metabolism in heifers. *J Anim Sci* 77:2523–2532, 1999
 33. Asarian L, Langhans W: Current perspectives on behavioural and cellular mechanisms of illness anorexia. *Int Rev Psychiatry* 17:451–459, 2005
 34. Haziot A, Ferrero E, Kontgen F, Hijiya N, Yamamoto S, Silver J, Stewart CL, Goyert SM: Resistance to endotoxin shock and reduced dissemination of gram-negative bacteria in CD14-deficient mice. *Immunity* 4:407–414, 1996
 35. Kitchens RL, Thompson PA: Modulatory effects of sCD14 and LBP on LPS-host cell interactions. *J Endotoxin Res* 11:225–229, 2005
 36. Haziot A, Chen S, Ferrero E, Low MG, Silber R, Goyert SM: The monocyte differentiation antigen, CD14, is anchored to the cell membrane by a phosphatidylinositol linkage. *J Immunol* 141:547–552, 1988
 37. Goyert SM, Ferrero E, Rettig WJ, Yenamandra AK, Obata F, Le Beau MM: The CD14 monocyte differentiation antigen maps to a region encoding growth factors and receptors. *Science* 239:497–500, 1988
 38. Moore KJ, Andersson LP, Ingalls RR, Monks BG, Li R, Arnaout MA, Golenbock DT, Freeman MW: Divergent response to LPS and bacteria in CD14-deficient murine macrophages. *J Immunol* 165:4272–4280, 2000
 39. Cipolletta C, Ryan KE, Hanna EV, Trimble ER: Activation of peripheral blood CD14+ monocytes occurs in diabetes. *Diabetes* 54:2779–2786, 2005
 40. Fernandez-Real JM, Broch M, Richart C, Vendrell J, Lopez-Bermejo A, Ricart W: CD14 monocyte receptor, involved in the inflammatory cascade, and insulin sensitivity. *J Clin Endocrinol Metab* 88:1780–1784, 2003
 41. Vyberg M, Ravn V, Andersen B: Pattern of progression in liver injury following jejunoileal bypass for morbid obesity. *Liver* 7:271–276, 1987
 42. Brun P, Castagliuolo I, Leo VD, Buda A, Pinzani M, Palu G, Martines D: Increased intestinal permeability in obese mice: new evidence in the pathogenesis of nonalcoholic steatohepatitis. *Am J Physiol Gastrointest Liver Physiol* 292:G518–G525, 2007
 43. Pappo I, Becovier H, Berry EM, Freund HR: Polymyxin B reduces cecal flora, TNF production and hepatic steatosis during total parenteral nutrition in the rat. *J Surg Res* 51:106–112, 1991
 44. Poggi M, Bastelica D, Gual P, Iglesias M, Grémeaux T, Knauf C, Peiretti F, Verdier M, Juhan-Vague I, Tanti J, Burcelin R, Alessi M: C3H/HeJ mice carrying a toll-like receptor 4 mutation are protected against insulin resistance that develops in white adipose tissue in response to a high-fat diet. *Diabetologia* 50:1267–1276, 2007
 45. Suganami T, Tanimoto-Koyama K, Nishida J, Itoh M, Yuan X, Mizuarai S, Kotani H, Yamaoka S, Miyake K, Aoe S, Kamei Y, Ogawa Y: Role of the toll-like receptor 4/NF- κ B pathway in saturated fatty acid-induced inflammatory changes in the interaction between adipocytes and macrophages. *Arterioscler Thromb Vasc Biol* 27:84–91, 2007
 46. Backhed F, Ley RE, Sonnenburg JL, Peterson DA, Gordon JI: Host-bacterial mutualism in the human intestine. *Science* 307:1915–1920, 2005
 47. Cani PD, Neyrinck AM, Maton N, Delzenne NM: Oligofructose promotes satiety in rats fed a high-fat diet: involvement of glucagon-like peptide-1. *Obes Res* 13:1000–1007, 2005